

*36th International Electric Vehicle Symposium and Exhibition (EVS36)
Sacramento, California, June 11-14, 2023*

Locating charging stations for shared autonomous electric vehicles with V2G operations in Brussels

Ona Van den bergh^{1,2}, Cedric De Cauwer^{1,3}, Lieselot Vanhaverbeke^{1,2}

Ona Van den bergh (corresponding author) ona.van.den.bergh@vub.be

¹*Electromobility Research Centre , Vrije Universiteit Brussel, Pleinlaan 2, 1050 Brussels, Belgium*

²*Business Technology and Operations department, Vrije Universiteit Brussel, Pleinlaan 2, 1050 Brussels, Belgium*

³*Electrical and Energy Engineering department, Vrije Universiteit Brussel, Pleinlaan 2, 1050 Brussels, Belgium*

Executive Summary

This paper proposes a multi-objective optimization model to locate charging stations for shared autonomous electric vehicles (SAEV) with vehicle-to-grid (V2G) operations. Mobility requirements, grid restrictions, and solar power density are included in the model. The model is applied to the Brussels road and distribution grid network to determine the optimal charging station locations. The results of this research show that considering the grid restrictions leads to a geographically more distributed allocation of charging stations. This coincides with a lower mean coverage of mobility demand. Next, the model is solved for different levels of importance for both the mobility part and the solar density part. A trade-off between both parts must be made by adequately choosing a weight to determine the importance for both parts. Varying this weight has an effect on the coverage of mobility demand and the mean solar density. Based on the analysis in this paper, an optimal trade-off is determined.

Keywords: optimization, charging, infrastructure, V2G (vehicle-to-grid), mobility system

1 Introduction

Shared autonomous electric vehicles (SAEVs) are a promising solution to several challenges facing the transportation industry, including alleviating traffic congestion and reducing greenhouse gas (GHG) emissions. The former is a result of the fact that SAEVs are designed to operate without human drivers and can be shared among multiple passengers, reducing the number of vehicles on the road [1, 2]. One SAEV can replace 3 to 13 conventional vehicles, depending on several factors such as vehicle range, level of charging, and population density. The latter is a result of the combination of electrification, ride-sharing, and autonomy. Research found through a complete Life Cycle Assessment that electric vehicles (EV) have the lowest CO₂ emissions amongst internal combustion engine vehicles (ICEV) and its alternatives [3]. Ride-sharing reduces the total vehicle kilometres travelled (VKT) [4]. This, in combination with the SAEV's smaller fleet and the energy efficient driving style of autonomous vehicles (AV) [5], leads to SAEVs reducing GHG emissions even further.

One of the significant advantages of SAEVs, besides reducing GHG emissions, is their potential to facilitate vehicle-to-grid (V2G) charging, a technology that allows electric vehicles to provide energy back to the grid when not in use. With V2G charging, SAEVs can act as mobile energy storage units, helping to balance the grid and increase the reliability of renewable energy sources (RES) such as wind and solar power [6].

Locating charging points for a SAEV fleet participating in V2G services is a great challenge. The infrastructure requirements associated with implementing these technologies, are threefold. Firstly, the allocation of charging infrastructure for SAEVs has an influence on the efficient routing of the fleet. We call this the mobility component. Secondly, the grid component implies that charging points must be integrated in the grid in locations where the grid is strong enough, since poor allocation could lead to grid problems such as voltage instability and increased power losses [7]. Thirdly, V2G can serve as a means to support the distribution grid in avoiding congestion, overloading, and assist in local balancing. These are V2G applications with a local component, which is why this must be taken into account in the location model. In previous research, elements were defined that are needed to be brought together in one location model to satisfy the three components of charging infrastructure requirements [6]. In this paper, we propose a location model for charging stations (CS) that incorporates these components. The rest of this paper is organized as follows. Section 2 refers to related work. The methodology and materials are presented in Section 3. In Section 4 the results are discussed, and Section 5 concludes the paper.

2 Related work

In our previous research [6, p.15] we defined six elements that need to be present in a location model for the charging infrastructure of SAEVs with V2G operations. These elements are the following: “Avoid placing too many CSs; Take restrictions on the power grid into consideration; Satisfy charging and mobility demand; Higher integration of renewable energy; Impose limits on the SOC to slow down battery degradation; Bring services to the grid.” In this paper, we propose a location model in which we include the first four elements. The following sections describe related work for each element.

2.1 Number of charging points

To avoid placing too many CSs (mainly to limit the cost), often a maximum number of chargers is imposed [8, 9, 10]. However, the question remains what this number should be, since battery range and charging power both affect the required number of charging stations for a certain fleet size. Based on previous research [8, 11, 12, 13] we created Table 1, which shows the ratio of SAEV fleet to number of charging points.

Battery capacity/range (kWh) (miles) (km)			Number of SAEVs per charging point						Reference	
			Charging power (kW)							
			±5	±7	±11	22	40	50	80	
12.5	<u>50</u>	80			6.5					[13]
17.5	<u>70</u>	112		3.2						[13]
20	<u>80</u>	128	1.9				2.4	32.5		[13, 11]
22.5	<u>90</u>	145			4.3					[13]
30	<u>124</u>	<u>200</u>		1.9						[12]
<u>40</u>	<u>160</u>	290				2.5-3.1			13.3	[11, 8]
<u>50</u>	<u>200</u>	320			2.5	2.8				[11, 8]

Table 1: The number of SAEVs per charging point for different battery ranges and charging powers. Underlined in the column ‘Battery capacity/range’ are the units that were used in the references. To complete the table, following ratio’s were used: 1 kWh for 4 miles battery range or 0.156kWh/km; 1.6 km for 1 mile [14, 15].

2.2 Restrictions on the power grid

To take restrictions on the grid into account, many researchers minimize power losses and limit voltage deviation [16, 17, 18]. Applying this to larger networks and/or practical cases requires detailed information of the distribution network, which is not always available [19]. Therefore, research usually uses the IEEE test feeders [20] as benchmark for power flow analyses. In order to introduce power availability on the distribution grid into this optimization, we opt to follow Distribution System Operator (DSO) guidelines to limit the roll-out of charging infrastructure to connection points on the three-phase 400V (3x400V+N) power supply and not the obsolete three-phase 230 V (3x230V), which is gradually being replaced. Connecting the charging infrastructure to the 400V voltage system allows for higher power availability for the EV drivers due to the three-phases (as opposed to a single phase in the conventional 230V voltage system, where a neutral conductor is absent) and reduces voltage unbalance, thermal stress and losses within the distribution grid.

2.3 Satisfy mobility demand

In order to account for mobility requirements, data on travel behaviour and mobility demand is needed. Travel data can be obtained by Origin-destination (OD) pairs. OD pairs represent the occurrence of trips and are therefore frequently used in mobility focused optimization problems. Examples of open data that can be used are StreetLight Data [21], National Household Travel Survey (NHTS) data [22], and Mobile Phone Trajectory data [12]. These data sources provide information about travel behaviour and can be used as direct input for optimization models, or as input for simulations.

It would be convenient for drivers to charge in the proximity of where they will start or just finished a trip. Therefore, it is a common assumption that origins and destinations of trips are suitable locations for charging. From OD pairs, the number of pick-up and drop-off (PUDO) points can be counted per area. These counts can be used in the location model. A possible strategy, used in [8, 23], is to maximize the covered PUDO points by placing CSs in the center of demand clusters. This problem formulation is called the maximal coverage location problem (MCLP). Another possibility, called the P-median model, is to minimize the distance between charging demand (often represented by the count of PUDO points) and CSs [8, 24, 9]. Vosooghi et al. compared the MCLP to the P-median model and found that the P-median model outperformed the MCLP in terms of in-vehicle person kilometers traveled. Gacias et al. [9] compared the P-median model to the demand-based model. In this model covered demand is maximized, while also limiting the distance to the nearest CS for every area. They concluded that the demand-based model outperformed the P-median model in terms of satisfied customers, taxi's operating time, and waiting time for an available charging station.

2.4 Higher integration of renewable energy sources

One of the advantages of V2G is their ability to increase the reliability of RES and thereby facilitate a higher integration of RES. Researchers have been looking into optimally locating RES and CSs simultaneously [25], locating solar powered charging stations [26], or locating CSs in a solar powered micro-grid [27]. They consider the solar power generation profile over time. However Sultan et al. [28] predict solar excess power generation spatially. They locate the CSs based on this spatial distribution such that the vehicles can absorb mid-day solar overgeneration.

3 Materials and methodology

Both the distribution and road transportation network are tied in the SAEV charging system. Both the network power load and the served charging demand for SAEVs can be impacted by locations of CSs. Therefore, we propose an optimization model which will maximize covered SAEV pick-up and drop-off points, maximize the solar power density, and simultaneously consider the availability of the distribution grid to install fast chargers.

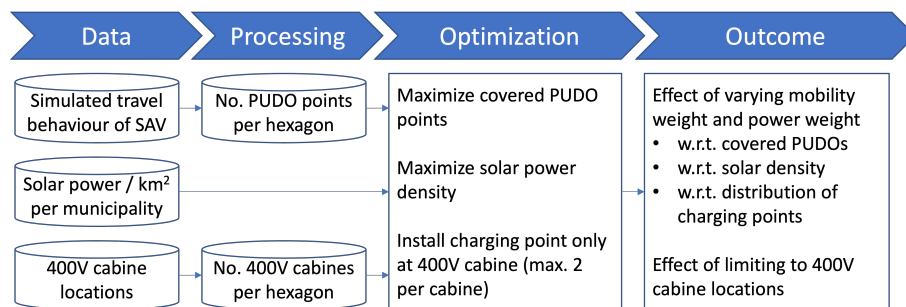


Figure 1: Conceptual framework

Li. et al [29] have simulated the substitution of private car trips in Brussels by a fleet of shared autonomous vehicles (SAV) under 10% of current demand. They only considered trips that start and end within Brussels. This means that trips starting from outside of Brussels are not accounted for. For this they found that a fleet of 1000 SAVs would suffice to provide a mobility service with a waiting time of less than 5 minutes. They have a large range and negligible refilling time. The trips from their simulation served as input data for this research.

However we must take into account that the simulation was accounted for non-electric SAVs. Since in this paper we will locate charging infrastructure for SAEVs, which are electric SAVs, we need to make a few notations. Firstly, the range of the SAEVs affects the needed number of chargers [1]. Secondly, the charge power affects the fleet size. To maintain the validity of the 1000 non-electric SAVs simulation,

we must account for these two effects. Therefore, we assume a battery range of 300km and a charging rate of 50kW.

We start by dividing Brussels into hexagons with an edge length of 174 meters, thereby creating a hexagonal grid. The hexagonal shape ensures that the distance from the centre to centre of each neighbouring hexagonal is equal. This type of grid has been proven to be more suitable in various types of research [30, 31].

3.1 Road transportation network

For the road transportation part, we suggest a variation of the MCLP used in [8, 23]. Our contribution to their model is that we will also decide on the numbers of charging points per chosen location, and not only on the locations itself. From the OD pairs, we count the number of PUDO locations of SAEVs per hexagon. PUDO locations are the locations where SAEVs finish one ride before picking up a new one. To avoid unnecessary detours, it would be convenient from a mobility point of view to install charging points at these locations.

To each hexagon $i \in H$ we assign an integer value x_i equal to the number of charging points located in this hexagon. The goal is to maximize the total covered PUDO points. We call a PUDO point ‘covered’ if a charging point is assigned to it. Despite the fact that in reality not every PUDO point would generate an actual charging demand, there is a proportional relation between number of PUDO points and charging demand. Therefore, a higher number of PUDO points in a certain hexagon would generate a higher charging demand and consequently more charging points are needed in this hexagon. Therefore, maximizing the total covered PUDO points mimics maximizing covered charging demand.

Vosooghi et al. [8] consider an area to be covered as soon as one CS is installed in this area. That means that according to their model, even in an area with very high charging demand, one CS would suffice to cover the complete area. However, when two charging requests occur simultaneously in an area with only one charging point, it is impossible to serve both charging requests. Hence, we believe that their assumption is not realistic. Therefore, we propose a coverage rate r_i relative to the ratio between the number of charging points installed x and the number of PUDO points c in this and neighbouring hexagons, as formulated in Equation (1). This formula is adapted from the one used in [8, 23], according to the argumentation above.

$$r_i = \frac{\overset{\text{number of charging points in } i^{\text{th}} \text{ hexagon}}{x_i}}{\underset{\text{number of PUDO points in } i^{\text{th}} \text{ hexagon}}{c_i} + \epsilon} + \frac{1}{2} \cdot \sum_{j \in N_i} \frac{x_j}{c_i + \epsilon} \quad (1)$$

↑
↑ *neighbouring hexagons of i^{th} hexagon*

In the calculation for the coverage rate, charging points installed in the considered hexagon are counted fully, and charging points installed in neighbouring hexagons are counted only half. To clarify, we provide an example depicted in Figure 2. The addition of the small value ϵ in the denominator of Equation (1) is to avoid dividing by zero in case no PUDO points are counted in a certain hexagon. The coverage rate can be interpreted as the extent to which charging points are linked to PUDO points. It represents a percentage of possible charging demand that will be covered. It would be desirable that hexagons with a high PUDO count, and thus a high possible charging demand, are equipped with more CSs and thereby will have a high coverage rate. However, the higher the PUDO count in a certain hexagon, the higher the required number of CSs to reach a certain coverage rate. As a result, installing CSs in hexagons with low PUDO counts typically leads to higher coverage rates. For this reason, we must keep in mind that coverage rate is not always a reliable parameter to assess the strength of a solution for CS allocation.

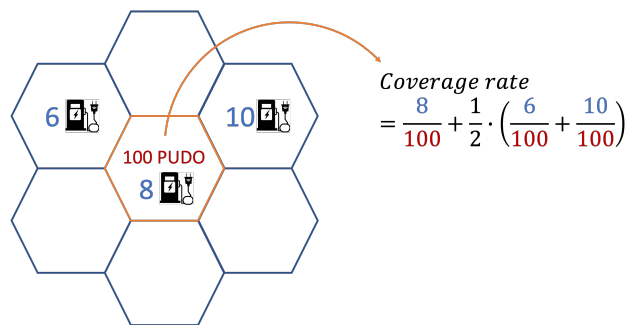


Figure 2: Illustration for the calculation of the coverage rate.

To retrieve a more reliable absolute number to represent the coverage in a hexagon, we can multiply its coverage rate with its number of PUDO points. The result of this multiplication is called the number of covered PUDOs. However, it should not be possible that a hexagon has more covered PUDOs than the number of PUDO points in this hexagon. Therefore, in the calculation of covered PUDOs, the coverage rate should be limited to maximum 1. For this reason, we define a new variable weight w . The weight of a hexagon w_i is equal to its coverage rate, but is limited to 1. This weight will be used in the objective function in our location model to calculate the covered PUDO points. As mentioned earlier, the goal is to maximize the total covered PUDO points. Finally a maximal number of CSs is defined as B . This number must be fixed beforehand and is based on prior work. The following maximal covering location problem is formed:

$$\begin{aligned} \text{maximize}_{x_i} \quad & \sum_{i \in H} c_i w_i & (2) \\ & \uparrow \text{weight of } i^{\text{th}} \text{ hexagon} \\ & \uparrow \text{set of hexagons} \end{aligned}$$

$$\text{subject to} \quad \sum_{i \in H} x_i < B \quad (3)$$

↑ maximal number of chargers

$$w_i \leq \min \left(1, \frac{x_i}{c_i + \epsilon} + \frac{1}{2} \cdot \sum_{j \in N_i} \frac{x_j}{c_j + \epsilon} \right) \quad \forall i \in H \quad (4)$$

↑ coverage rate of i^{th} hexagon

$$x_i \text{ is integer} \quad \forall i \in H \quad (5)$$

The decision variable x_i is the number of charging points to be installed in hexagon i . The objective function (2) maximizes the total number of captured PUDO points. Constraint (9) imposes a maximum number of CSs, and constraint (10) ensures that the weight of each hexagon cannot be greater than 1.

3.2 Distribution network

Next to the road transportation network, we also want to take the grid into account. As discussed in subsection 2.2, charging at 400 volt cabins facilitates some advantages, such as faster charging and discharging rates, enabling more efficient and effective V2G operations. Therefore, we limit the potential locations for CSs to there where a 400V cabin is located. In a conversation with the DSO of Brussels, it was indicated that a maximum load capacity of 100kW is possible per cabin. Because we will work with fast chargers that go up to 50kW, we limit ourselves to 2 charging points per cabin, which leads to the following constraint:

$$x_i \leq 2 y_i \quad \forall i \in H \quad (6)$$

↑ number of 400V cabins in i^{th} hexagon

3.3 Power generation density

To maximize the potential of RES integration in the grid, we aim to install CSs at locations with an excess of solar generation. Due to lack of power excess data and power load data, we estimate the excess according to the power generation density. We have access to data that shows the solar power density per municipality in Brussels [32], as shown in Figure 3c. We assume that a higher solar power generation per area results in a higher probability of a solar power excess. For this reason, we want our model to place CSs in areas with a high solar power density. To reach this, we maximize the ‘covered’ power density with objective function 7.

$$\text{maximize}_{x_i} \quad \sum_{i \in H} x_i p_i \quad (7)$$

↑ solar power density in i^{th} hexagon

3.4 Final location model

In our final model, we combine the mobility objective function and the power density objective function by constructing one weighted objective function. Therefore, we first normalize the PUDO counts (\hat{c}) and solar power density (\hat{p}), such that both vectors are equally considered. The mobility objective function is assigned weight w_m , and the power density objective function is assigned weight w_p . Also the mobility constraints and the grid constraint are added to model. Our final model is presented below.

$$\begin{aligned} & \underset{x_i}{\text{maximize}} && w_m \sum_{i \in H} \hat{c}_i w_i + \sum_{i \in H} x_i \hat{p}_i && (8) \end{aligned}$$

$$\begin{aligned} & \text{subject to} && \sum_{i \in H} x_i < B && (9) \end{aligned}$$

$$w_i \leq \min \left(1, \frac{x_i}{c_i + 0.01} + \frac{1}{2} \cdot \sum_{j \in N_i} \frac{x_j}{c_j + 0.01} \right) \quad \forall i \in H \quad (10)$$

$$x_i \leq 2y_i \quad \forall i \in H \quad (11)$$

$$x_i \text{ is integer} \quad \forall i \in H \quad (12)$$

4 Results

We first divided Brussels into 1783 hexagons with an average edge length of 174m. After that, it was possible to visualize our data on the hexagonal grid.

We used three types of input data: 14 975 PUDO locations, later converted to PUDO counts per hexagon, respectively visualized in Figures 3a and 3b; the locations of the 400V cabins in Brussels; and the solar power density per municipality, visualized in Figure 3c.

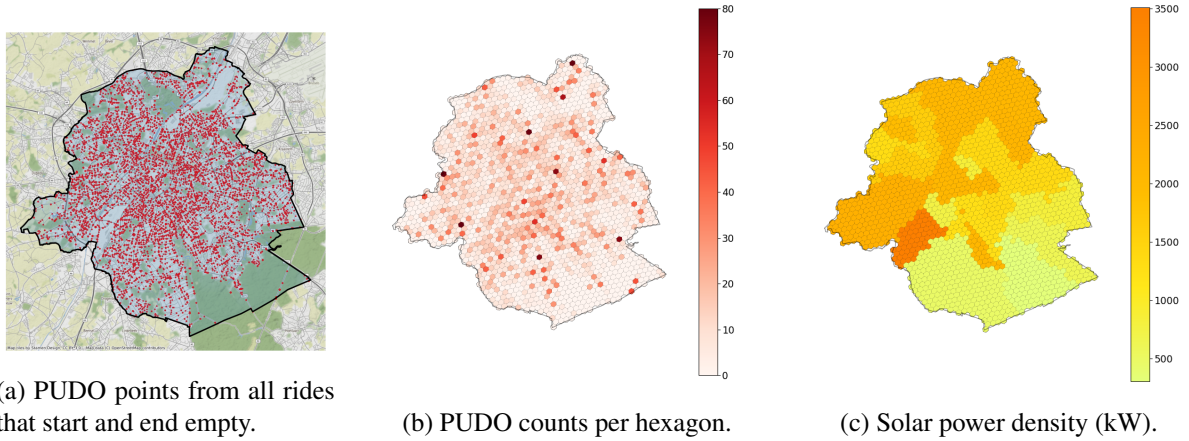


Figure 3: Input data visualization.

Currently, the mean range of EVs is around 300 km [33]. In this paper, we aim to install fast-chargers which can go up to 50kW. As shown in Table 1, previous research found a wide range for the ratio of SAEV fleet to number of charging points. It is therefore not easy to estimate the number of we would need in Brussels for a fleet of 1000 SAEVs. However, we see that numbers around 2.5 occur several times for higher ranges and charging powers, apart from some outlying numbers. Therefore, we conclude that this ratio, which would match with 400 charging points for a fleet of 1000 SAEVs, is a good starting point for our case study.

4.1 Add grid constraint

Figure 4 shows the effect of limiting the potential CS locations to there where a 400V cabine is installed. We see that charging points are forced to be more dispersed, due to the limit of 2 charging points per cabine. Figure 5 shows the effect of adding the grid constraint, and thereby moving from a situation where CSs are located very densely in high demand hexagons to a geographically slightly more dispersed distribution of CSs. As mobility is still the only component in the objective function, CSs are still located in hexagons with high PUDO counts. However, due to the grid constraint less CSs can be installed per hexagon, lowering the mean¹ coverage rate from 58% to 37%, as shown in Figure 5a. The higher dispersion means that more hexagons will be equipped with at least one CS and thereby retrieve a non-zero coverage rate. From now on we call hexagons with a non-zero coverage rate ‘equipped hexagons’. The

¹This mean is calculated based only on equipped hexagons.

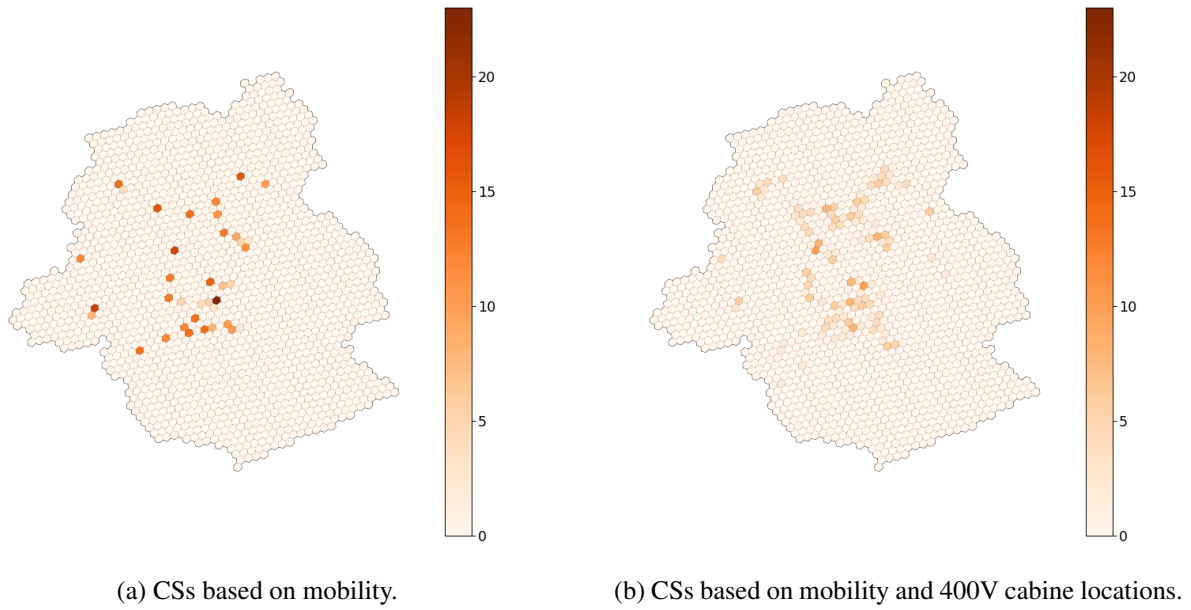


Figure 4: Optimal solution for charging points in Brussels **(a)** with only PUDOs taken into account, and **(b)** with PUDOs taken into account together with the locations of 400V cabins.

number of equipped hexagons increased from 192 to 345. As a result, despite the lower mean coverage rate, the total coverage (the sum over all coverage rates) increased. However, although the total coverage increased, both the mean and total covered PUDOs decreased, as shown in Figure 5b. Since the number of covered PUDOs represents the extent to which charging demand is served, these values should be as high as possible.

We conclude that a geographically higher coverage – which naturally happens by adding the grid constraint – does not mean a better solution in terms of mobility requirements, as the mean coverage rate decreases and both mean and total covered PUDOs decrease as well. This means that there is a lower extent to which CSs are linked to PUDOs and there will be a lower satisfaction of charging demand.

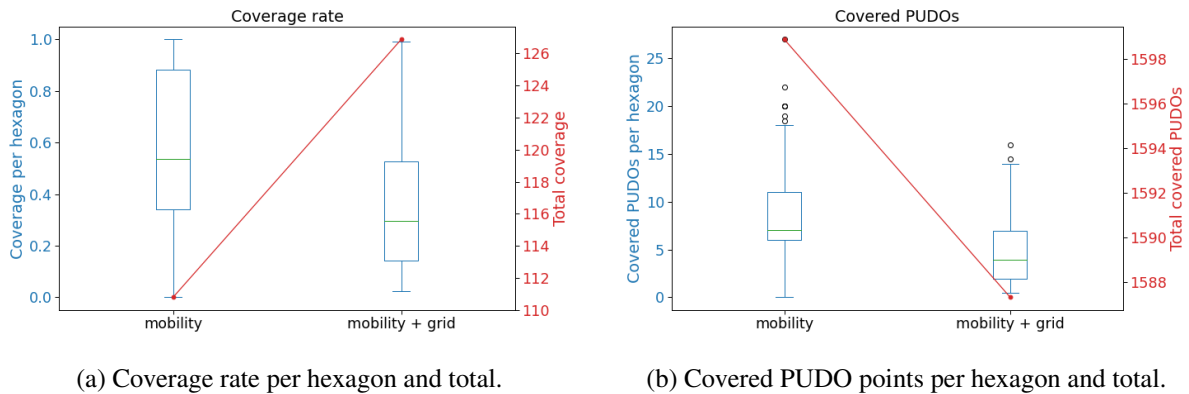


Figure 5: Effect of adding the grid constraint 6 on **(a)** coverage rate, and **(b)** covered PUDO points. Only equipped hexagons (i.e. hexagons with a non-zero coverage rate) are considered in these box-plots.

4.2 Vary mobility weight and power weight

Figure 6 shows the optimal sizing and siting of CSs for varying mobility and power weights w_m and w_p . It is clear that for higher w_p , the charging points are located more towards the West of Brussels, which has the highest solar power density. With increasing w_m , the charging points locations shift more

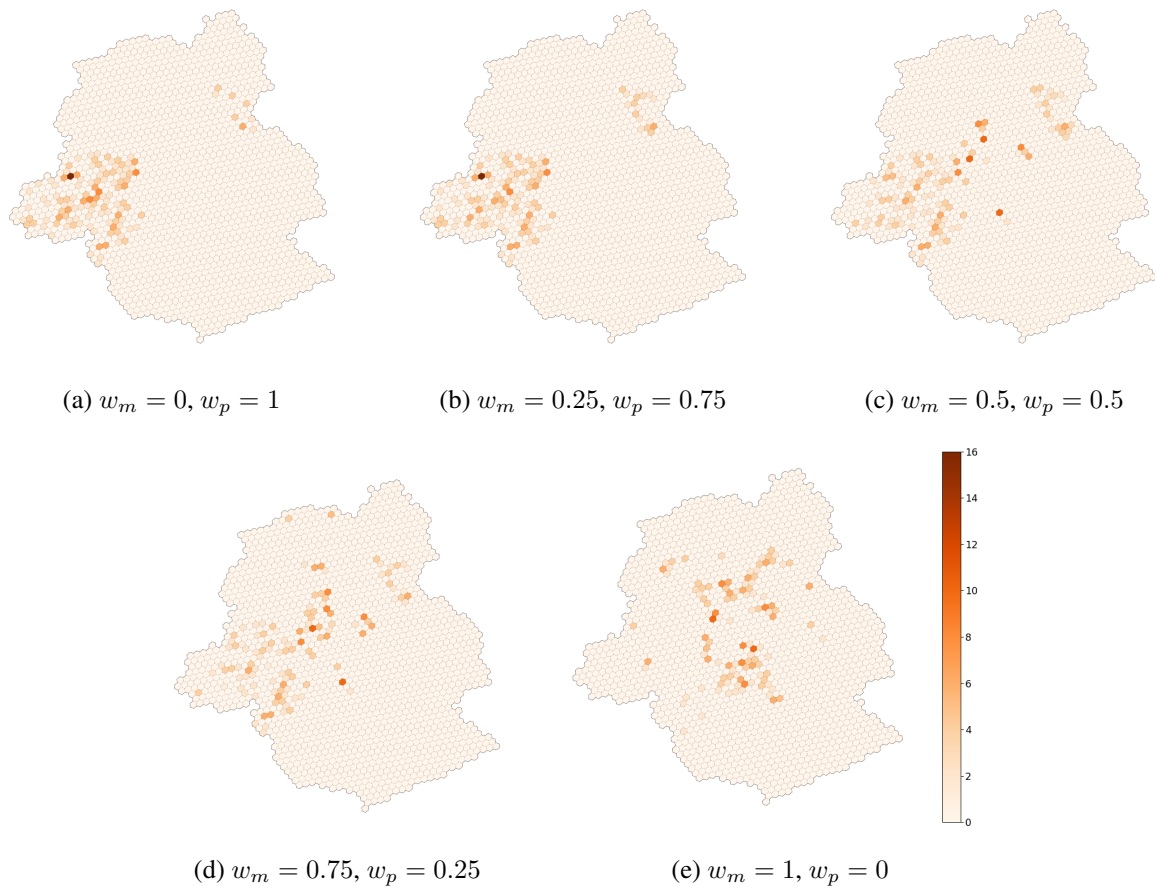


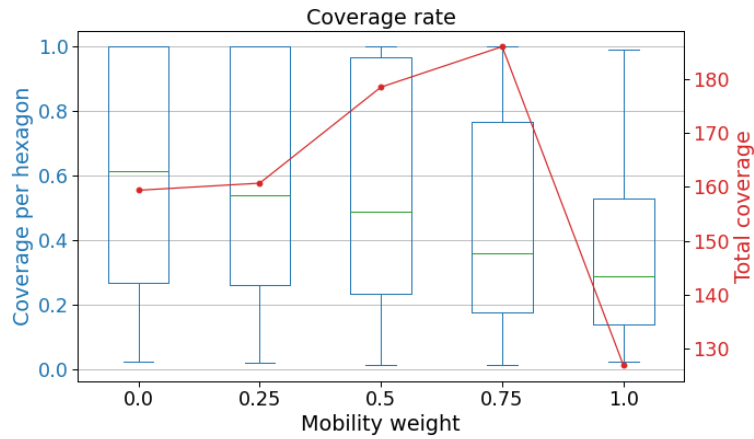
Figure 6: Optimal solution for charging stations in Brussels with varying weights w_m for the mobility objective function and w_p for the power density objective function.

towards the center of Brussels, which has more mobility demand. The effect of this shifting is analysed based on three variables: coverage rate, covered PUDO points, and solar power density.

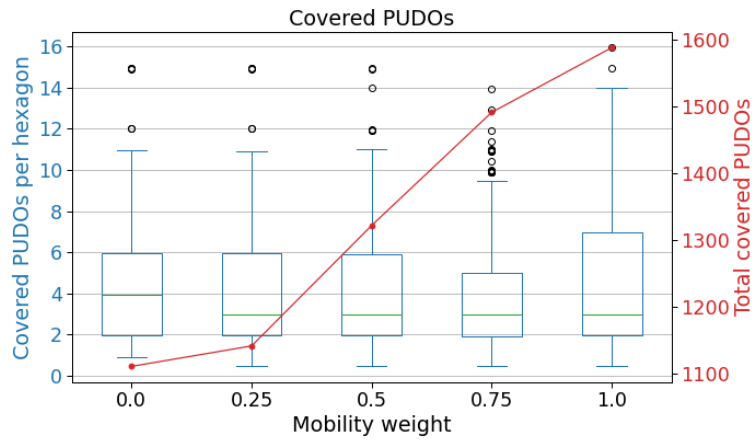
By the shift we see in Figure 6, we can conclude that these two types of hexagons do not coincide. This means that for lower w_m and higher w_p , CSs are located in hexagons with lower PUDO counts. As a result, the mean coverage rate will be higher for lower w_m and vice versa, since coverage rate is inversely proportional to PUDO count. This trend can also be noticed in Figure 7a. However, the total coverage increases for w_m going from 0 to 0.75. This follows from the fact that the number of equipped hexagons for mobility weights 0, 0.25, 0.5, and 0.75 are respectively 266, 279, 327, 402. Finally for $w_m = 1$, the 349 covered hexagons add up to the lowest total coverage rate of all scenario's. The narrow box in the box-plot of this scenario shows that the coverage rates of the equipped hexagons are more concentrated around the lower values. This is because charging points are located in high demand area's, with high PUDO counts, where coverage rates are typically lower. Therefore, it is important to also look at the absolute numbers, depicted in Figure 7b. We observe that the total number of covered PUDO points increases at every step with w_m approaching 1. This is not surprising, as for each increase in w_m the total number of covered PUDO points weights more in the objective function (8), which is maximized.

Finally we analyse the effect of the shift in CS locations on solar power density based on Figure 8. The mean and total solar density decrease slightly as w_m increases from 0 to 0.75. However the difference is only very small. For $w_m = 1$ (thus $w_p = 0$) there is a significant drop both in mean and total solar density. From this Figure it is clear that as long that solar power density is considered in the objective function ($w_p \neq 0$), the exact value of w_p is not too influential on the final mean and total solar density.

From these results, we can conclude that the mobility part of the model locates charging points in area's of high PUDO count. This leads to rather low mean and total coverage rates. However, a high total covered number of PUDO points is reached, indicating a high satisfaction of charging demand. On the other hand, the power density part tends to densely concentrate the CS locations in the high solar powered area's, where PUDO counts are lower. This leads to the highest mean coverage rate and the highest mean



(a) Coverage rate per hexagon and total.



(b) Covered PUDO points per hexagon and total.

Figure 7: Effect of varying w_m and w_p on (a) coverage rate, and (b) covered PUDO points. Only equipped hexagons (i.e. hexagons with a non-zero coverage rate) are considered in these box-plots.

solar power density However, the total coverage stays rather low due to the low number of equipped hexagons, and the total number of covered PUDOs reaches a minimum.

Therefore it is important to choose w_m and w_p carefully in order to reach a balance between dispersion, locations in high PUDO counts area's, and highly solar powered area's. In the case study presented in this paper, a mobility weight of $w_m = 0.75$ would be advisable. Firstly, this weight leads to the highest total coverage rate. Also, the total number of covered PUDO points that matches with this weight reaches 93% of the highest possible total linked to scenario $w_m = 1$. Finally the mean solar power density for $w_m = 0.75$ is very close to the optimal value at scenario $w_m = 0$.

5 Conclusion

In this paper a multi-objective optimization model is proposed to locate charging stations for SAEVs with V2G operations. Mobility requirements, grid restrictions, and solar power density were included in the model, which was applied to the Brussels road and distribution grid network. First, the addition of the grid constraint that requires that CSs are located at 400V cabins, was analyzed. The limit of installing at most two fast-charging points per cabin leads to a higher dispersity of CSs. Although this results in a higher total coverage, the mean and total number of covered PUDO points decreased. This means that the satisfaction of charging demand would be lower. In a second part of this study, the optimal sizing and siting of CSs for varying mobility and power weights have been analyzed. From the moment that the weight of solar density is 0.25, further increasing the weight only has low impact on the mean and total

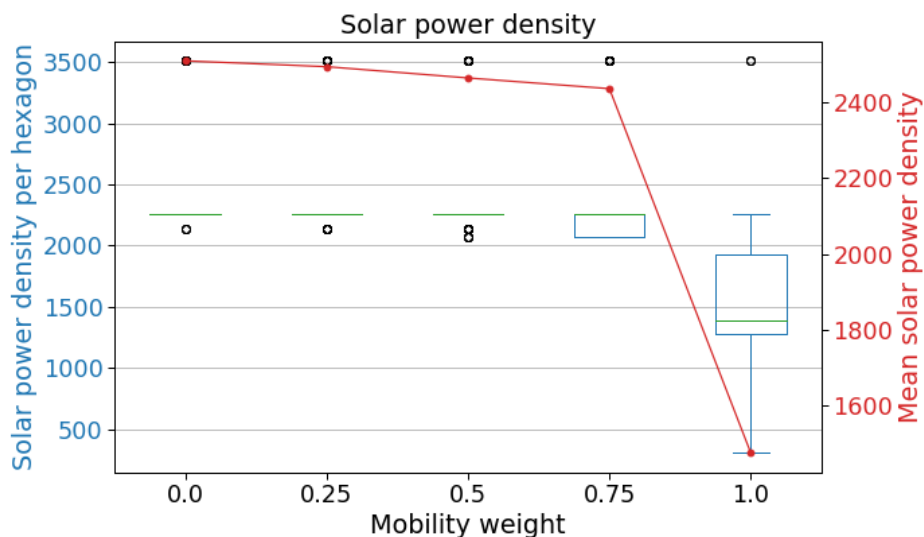


Figure 8: Solar power density for varying w_m and w_p . Only equipped hexagons (i.e. hexagons with a non-zero coverage rate) are considered in these box-plots.

solar density. Varying the weights has however a large impact on the coverage of mobility demand. The results show that the mobility model (the model with mobility weight $w_m = 1$) tends to locate charging points in high PUDO count areas, while the power density model (the model with mobility weight $w_m = 0$) concentrates the CS locations too much in highly solar-powered areas, both leading to a low total coverage rate (due to a low number of covered hexagons for $w_m = 0$, and due to a low mean coverage rate for $w_m = 1$). Therefore, it is important to carefully choose the w_m and w_p ($1 - w_m$) values to strike a balance between dispersity, locations in high PUDO count areas, and highly solar-powered areas.

This study found that a mobility weight of $w_m = 0.75$ would be advisable, as it leads to the highest total coverage rate while the total number of covered PUDO points does not deviate much from the highest total found at scenario $w_m = 1$. Additionally, the mean and total solar power density for $w_m = 0.75$ are close to the optimal values found at scenario $w_m = 0$. Overall, the study highlights the need for a balanced approach when designing the optimal siting of CSs for SAEVs with V2G in urban areas. These results can be useful for planners and policymakers to optimize the siting and sizing of CSs for sustainable and efficient charging infrastructure.

The future research that we are planning to undertake, includes following three aspects. Firstly, we want to adapt our model in such a way to avoid clustering charging points too densely in area's with high PUDO points by imposing a maximal distance between each PUDO point and the nearest CS. Secondly, to determine the optimal weights for the objective function, a trade-off must be made between the final mean solar power density and the total covered PUDO points. We want to assign a score to each location solution in order to formally decide on this trade-off. Finally, in our current model the mobility demand is only analyzed spatially. In the future, we want to add a temporal component.

Acknowledgments

We would like to acknowledge Sibelga for providing the dataset with the locations of the 400V cabins in Brussels, used in this research.

References

- [1] O. Van den bergh, C. De Cauwer, and L. Vanhaverbeke, "Vehicle-to-grid strategy for shared autonomous electric vehicles : A review of the charging infrastructure 's impacts on energy and mobility," in *35th International Electric Vehicle Symposium and Exhibition (EVS35)*, 2022, pp. 1–25.
- [2] J. Li, E. Rombaut, and L. Vanhaverbeke, "A systematic review of agent-based models for autonomous vehicles in urban mobility and logistics: Possibilities for integrated simulation

- models,” *Computers, Environment and Urban Systems*, vol. 89, no. May, p. 101686, 2021. [Online]. Available: <https://doi.org/10.1016/j.compenvurbsys.2021.101686>
- [3] J. Van Mierlo, M. Messagie, and S. Rangaraju, “Comparative environmental assessment of alternative fueled vehicles using a life cycle assessment,” *Transportation Research Procedia*, vol. 25, pp. 3435–3445, 2017.
- [4] European Environment Agency, *Electric vehicles from life cycle and circular economy perspectives*, 2018, no. 13.
- [5] J. M. Greenwald and A. Kornhauser, “It’s up to us: Policies to improve climate outcomes from automated vehicles,” *Energy Policy*, vol. 127, pp. 445–451, 4 2019.
- [6] O. Van den bergh, S. Weekx, C. De Cauwer, and L. Vanhaverbeke, “Locating Charging Infrastructure for Shared Autonomous Electric Vehicles and for Vehicle-to-Grid Strategy : A Systematic Review and Research Agenda from an Energy and Mobility Perspective,” *World Electric Vehicle Journal*, vol. 14, no. 56, 2023. [Online]. Available: <https://doi.org/10.3390/wevj14030056>
- [7] S. Deb, K. Tammi, X. Z. Gao, K. Kalita, and P. Mahanta, “A Hybrid Multi-Objective Chicken Swarm Optimization and Teaching Learning Based Algorithm for Charging Station Placement Problem,” *IEEE Access*, vol. 8, pp. 92 573–92 590, 2020.
- [8] R. Vosooghi, J. Puchinger, J. Bischoff, M. Jankovic, and A. Vouillon, “Shared autonomous electric vehicle service performance: Assessing the impact of charging infrastructure,” *Transportation Research Part D: Transport and Environment*, vol. 81, no. May 2019, 2020.
- [9] B. Gacias and F. Meunier, “Design and operation for an electric taxi fleet,” *OR Spectrum*, vol. 37, no. 1, pp. 171–194, 2015.
- [10] S. Wang, Z. Y. Dong, F. Luo, K. Meng, and Y. Zhang, “Stochastic Collaborative Planning of Electric Vehicle Charging Stations and Power Distribution System,” *IEEE Transactions on Industrial Informatics*, vol. 14, no. 1, pp. 321–331, 2018.
- [11] T. D. Chen, K. M. Kockelman, and J. P. Hanna, “Operations of a shared, autonomous, electric vehicle fleet: Implications of vehicle & charging infrastructure decisions,” *Transportation Research Part A: Policy and Practice*, vol. 94, pp. 243–254, 2016. [Online]. Available: <http://dx.doi.org/10.1016/j.tra.2016.08.020>
- [12] H. Miao, H. Jia, J. Li, and T. Z. Qiu, “Autonomous connected electric vehicle (ACEV)-based car-sharing system modeling and optimal planning: A unified two-stage multi-objective optimization methodology,” *Energy*, vol. 169, pp. 797–818, 2019. [Online]. Available: <https://doi.org/10.1016/j.energy.2018.12.066>
- [13] G. S. Bauer, J. B. Greenblatt, and B. F. Gerke, “Cost, energy and environmental impact of automated electric taxi fleets in Manhattan,” *Angewandte Chemie International Edition*, 6(11), 951–952., 2018.
- [14] E. X. Way, <https://evcharging.enelx.com/resources/blog/666-how-far-can-electric-cars-go-on-one-charge>, accessed on 2023-03-22.
- [15] E. Matters, <https://www.energymatters.com.au/renewable-news/your-guide-to-calculating-the-energy-consumption-of-an-electric-vehicle/>, accessed on 2023-03-22.
- [16] M. Bilal and M. Rizwan, “Integration of electric vehicle charging stations and capacitors in distribution systems with vehicle-to-grid facility,” *Energy Sources, Part A: Recovery, Utilization and Environmental Effects*, 2021.
- [17] O. Rahbari, M. Vafaeipour, N. Omar, M. A. Rosen, O. Hegazy, J. M. Timmermans, S. Heibati, and P. V. D. Bossche, “An optimal versatile control approach for plug-in electric vehicles to integrate renewable energy sources and smart grids,” *Energy*, vol. 134, pp. 1053–1067, 2017. [Online]. Available: <http://dx.doi.org/10.1016/j.energy.2017.06.007>
- [18] R. Chakraborty, D. Das, and P. Das, “Optimal Placement of Electric Vehicle Charging Station with V2G Provision using Symbiotic Organisms Search Algorithm,” *2022 IEEE International Students’ Conference on Electrical, Electronics and Computer Science, SCEECS 2022*, no. 2, pp. 8–13, 2022.
- [19] R. Li, C. Gu, F. Li, G. Shaddick, and M. Dale, “Development of low voltage network templates-part i: Substation clustering and classification,” *IEEE Transactions on Power Systems*, vol. 30, no. 6, pp. 3036–3044, Nov. 2015.

- [20] K. P. Schneider, B. A. Mather, B. C. Pal, C. W. Ten, G. J. Shirek, H. Zhu, J. C. Fuller, J. L. Pereira, L. F. Ochoa, L. R. De Araujo, R. C. Dugan, S. Matthias, S. Paudyal, T. E. McDermott, and W. Kersting, “Analytic Considerations and Design Basis for the IEEE Distribution Test Feeders,” *IEEE Transactions on Power Systems*, vol. 33, no. 3, pp. 3181–3188, 2018.
- [21] J. Luke, M. Salazar, R. Rajagopal, and M. Pavone, “Joint Optimization of Autonomous Electric Vehicle Fleet Operations and Charging Station Siting,” *IEEE Conference on Intelligent Transportation Systems, Proceedings, ITSC*, vol. 2021-Septe, pp. 3340–3347, 2021.
- [22] C. J. Sheppard, G. S. Bauer, B. F. Gerke, J. B. Greenblatt, A. T. Jenn, and A. R. Gopal, “Joint Optimization Scheme for the Planning and Operations of Shared Autonomous Electric Vehicle Fleets Serving Mobility on Demand,” *Transportation Research Record*, vol. 2673, no. 6, pp. 579–597, 2019.
- [23] J. Asamer, M. Reinthaler, M. Ruthmair, M. Straub, and J. Puchinger, “Optimizing charging station locations for urban taxi providers,” *Transportation Research Part A: Policy and Practice*, vol. 85, pp. 233–246, 2016. [Online]. Available: <http://dx.doi.org/10.1016/j.tra.2016.01.014>
- [24] M. Ravlić, T. Erdelić, and T. Carić, “Optimizing charging station locations for fleet of electric vehicles using Multi-Source Weber Problem,” *Proceedings Elmar - International Symposium Electronics in Marine*, no. September, pp. 111–114, 2016.
- [25] M. R. Mozafar, M. H. Moradi, and M. H. Amini, “A simultaneous approach for optimal allocation of renewable energy sources and electric vehicle charging stations in smart grids based on improved GA-PSO algorithm,” *Sustainable Cities and Society*, vol. 32, no. November 2016, pp. 627–637, 2017.
- [26] F. Ahmad, M. Khalid, and B. K. Panigrahi, “An enhanced approach to optimally place the solar powered electric vehicle charging station in distribution network,” *Journal of Energy Storage*, vol. 42, no. August, p. 103090, 2021.
- [27] K. Gupta, R. Achathuparambil Narayanankutty, K. Sundaramoorthy, and A. Sankar, “Optimal location identification for aggregated charging of electric vehicles in solar photovoltaic powered microgrids with reduced distribution losses,” *Energy Sources, Part A: Recovery, Utilization, and Environmental Effects*, pp. 1–16, 3 2020.
- [28] V. Sultan, H. Bitar, A. Alzahrani, and B. Hilton, “Electric Vehicles Charging Infrastructure Integration Into The Electric Grid Considering The Net Benefits To Consumers,” *7th International Conference on Smart Grids, Green Communications and IT Energy-aware Technologies (ENERGY)*, no. c, pp. 21–26, 2017.
- [29] J. Li, E. Rombaut, and L. Vanhaverbeke, “Simulation of Shared Autonomous Vehicles Operations with Relocation Considering External Traffic : Case Study of Brussels,” in *The 12th International Workshop on Agent-based Mobility, Traffic and Transportation Models, Methodologies and Applications (ABMTrans 2023)*, vol. 00, 2023.
- [30] M. Apte, Y. Agarwadkar, S. Azmi, and A. B. Inamdar, “Understanding grids and effectiveness of hexagonal grid in spatial domain,” *International Journal of Computer Applications*, vol. 1, no. February, pp. 25 – 27, 2012.
- [31] C. P. Birch, S. P. Oom, and J. A. Beecham, “Rectangular and hexagonal grids used for observation, experiment and simulation in ecology,” *Ecological Modelling*, vol. 206, no. 3-4, pp. 347–359, 2007.
- [32] Datastore, <https://datastore.brussels/web/data/dataset/043c9a7b-b1ff-4982-8c3b-643bed04872f>, accessed on 2023-03-22.
- [33] E. V. Database, <https://ev-database.org/cheatsheet/range-electric-car>, accessed on 2023-03-22.

Presenter Biography



Ona Van den bergh graduated in June 2021 as a Master of Science in Mathematics at the University of Antwerp (UA). She has a strong interest in (statistical) data science and optimization methods. In September 2021 she started as a PhD researcher and teaching assistant at the Vrije Universiteit Brussel (VUB) at the BUTO (Business Technology and Operations) department in the MOBI (Electromobility research centre) research group under supervision of prof. dr. Lieselot Vanhaverbeke. Her research activities are on autonomous electric mobility.